

Metal–organic frameworks in seconds *via* selective microwave heating†

Andrea Laybourn,<sup>\*ab</sup> Juliano Katrib,<sup>b</sup> Rebecca S. Ferrari-John,<sup>id b</sup> Christopher G. Morris,<sup>ac</sup> Sihai Yang,<sup>ac</sup> Ofonime Udoudo,<sup>b</sup> Timothy L. Easun,<sup>id ad</sup> Chris Dodds,<sup>b</sup> Neil R. Champness,<sup>id \*a</sup> Samuel W. Kingman<sup>\*b</sup> and Martin Schröder<sup>id \*ac</sup>

Cite this: *J. Mater. Chem. A*, 2017, 5, 7333

Received 17th February 2017  
Accepted 6th March 2017

DOI: 10.1039/c7ta01493g

rsc.li/materials-a

Synthesis of metal–organic framework (MOF) materials *via* microwave heating often involves shorter reaction times and offers enhanced control of particle size compared to conventional heating. However, there is little understanding of the interactions between electromagnetic waves and MOFs, their reactants, and intermediates, all of which are required for successful scale-up to enable production of commercially viable quantities of material. By examining the effect of average absorbed power with a constant total absorbed energy to prepare MIL-53(Al) we have defined a selective heating mechanism that affords control over MOF particle size range and morphology by altering the microwave power. This is the first time a selective mechanism has been established for the preparation of MOFs *via* microwave heating. This approach has been applied to the very rapid preparation of MIL-53(Al)*ta* (62 mg in 4.3 seconds) which represents the fastest reported synthesis of a MOF on this scale to date.

Metal–organic frameworks (MOFs) are highly porous crystalline materials consisting of metal ions or clusters bridged by organic ligands,<sup>1</sup> and their value arises from the void space within their structure (up to 90%),<sup>2</sup> which drives applications in gas storage and separation,<sup>3</sup> catalysis,<sup>4</sup> sensors,<sup>5</sup> and as supercapacitors.<sup>6</sup> Typically MOFs are prepared by solvothermal batch reactions whereby the reactants are heated above the boiling point of the solvent and retained under autogenous pressure for up to one week.<sup>7</sup> The duration and energy requirement of these reactions has led to a restriction in the adoption of MOFs for industrial applications owing to their high product cost. A critical need exists for technologies that reduce the time and cost of manufacture of MOFs<sup>8</sup> in order for their industrial potential to be fully realised.

Alternative synthetic routes to MOFs include mechanochemical,<sup>9</sup> electrochemical,<sup>10</sup> sonochemical,<sup>11</sup> and microwave<sup>12</sup> methods. Microwave heating is an extremely promising technology for MOF synthesis as it potentially offers shorter reaction times,<sup>13</sup> control over crystallite size,<sup>13,14</sup> and more energy

efficiency compared to conventional heating.<sup>15</sup> Many of the approaches for microwave synthesis of MOFs provide little understanding of the effect of microwave energy upon the bulk reaction mixture and simply use the average temperature of the reaction mixture as a key indicator.<sup>14,16</sup> There is also insufficient knowledge of parameters that are essential for scale-up. These parameters include (i) dielectric properties, defining the efficiency of power coupling and distribution of the electric field within the heating cavity; (ii) penetration depth and (iii) power density in the heated phase. Such information is crucially important when scale-up is considered as all of these variables underpin the design of large scale process systems. Failure to determine this fundamental information ultimately leads to failure in scale-up from the laboratory to industrial scale.

We report the effect of microwave heating to produce MIL-53(Al) (MIL = Materials Institute Lavoisier).<sup>17</sup> MIL-53(Al) was chosen since reaction kinetics in solution<sup>18</sup> and its properties<sup>19</sup> are well understood. We have determined<sup>20</sup> that aqueous M(III) salts are strong microwave absorbers (dielectric losses above 35), whereas the ligand, H<sub>2</sub>BDC (terephthalic acid), exhibits little interaction with the electric field at microwave frequencies (dielectric losses below 0.03) indicative of a selective heating process. We have now constructed a single mode standing wave microwave applicator capable of housing a high-pressure vessel (Fig. 1). This allows superimposition of the electric field maximum on the reaction mixture within the batch reactor, thus ensuring the maximum amount of microwave energy is being absorbed by the reaction mixture during treatment. The position of electric field is particularly important as the power density

<sup>a</sup>School of Chemistry, University of Nottingham, Nottingham NG7 2RD, UK. E-mail: Andrea.Laybourn@nottingham.ac.uk; Neil.Champness@nottingham.ac.uk

<sup>b</sup>Faculty of Engineering, University of Nottingham, Nottingham NG7 2RD, UK. E-mail: Sam.Kingman@nottingham.ac.uk

<sup>c</sup>School of Chemistry, University of Manchester, Oxford Road, Manchester M13 9PL, UK. E-mail: M.Schroder@manchester.ac.uk

<sup>d</sup>School of Chemistry, Cardiff University, Main Building, Park Place, Cardiff, CF10 3AT, UK

† Electronic supplementary information (ESI) available. See DOI: 10.1039/c7ta01493g



(process by which heat is generated from electromagnetic energy) is proportional to the electric field squared:

$$P_d = 2\pi f \epsilon_0 \epsilon'' E^2$$

where  $P_d$  is power density ( $\text{W m}^{-3}$ ),  $f$  is frequency (Hz),  $\epsilon_0$  is permittivity of free space,  $\epsilon''$  is the dielectric loss, and  $E$  is electric field strength in the material ( $\text{V m}^{-1}$ ).<sup>21</sup> Using this approach we have, for the first time, quantified experimentally the amount of energy absorbed by the MOF reaction mixture thus allowing investigation of energies required to reach desired reaction temperatures derived from theoretical calculation. We report the effect of power at fixed energy on the yield and properties (morphology, particle size, porosity) of MIL-53(Al) and demonstrate the synthesis of MOFs with the fastest production rate (62 mg in 4.3 seconds) in bulk reported to date.

## Experimental section

### General procedure for the investigation of microwave heating mechanism

$[\text{Al}_2(\text{SO}_4)_3] \cdot 18\text{H}_2\text{O}$  (0.77 g, 1.2 mmol), terephthalic acid (0.19 g, 1.2 mmol) and deionized water (6.7 mL) were mixed in a Teflon cup which was placed into a microwavable acid digestion vessel (Parr Instruments). The sealed reaction mixture was positioned in a purpose-built single mode microwave cavity behind a blast screen. The microwave power and reaction time were varied according to Table S3† in order to apply a target energy of 21 kJ to the reaction mixture (or 56  $\text{kJ mol}^{-1}$  based on water). The value of 21 kJ represents the theoretical amount of energy required to heat 6.7 mL of water to 220 °C (Table S1†), which has been determined as the temperature in which the as-synthesised phase of MIL-53(Al), denoted as MIL-53(Al)*ta*, forms in the conventional heating process.<sup>22</sup>

The electric field was pre-matched to the reaction mixture using an automatic 3-stub tuner (S-TEAM).<sup>23</sup> The 3-stub tuner was also used to measure the forward and reflected power from which

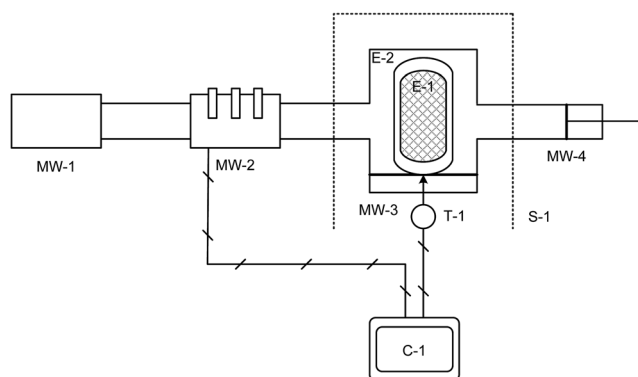


Fig. 1 Schematic of purpose-built single mode microwave system. Labels are assigned in Table S2 in ESI.† C-1: PC controller; E-1: Teflon cup for microwavable acid digestion vessel (Parr Instruments); E-2: outer section of microwavable acid digestion vessel (Parr Instruments); MW-1: Microwave generator; MW-2: Automatic 3-stub tuner; MW-3: Microwave applicator/cavity section; MW-4: sliding short; S-1: Lexan shield (blast-safe); T-1: Optris CT IR sensor.

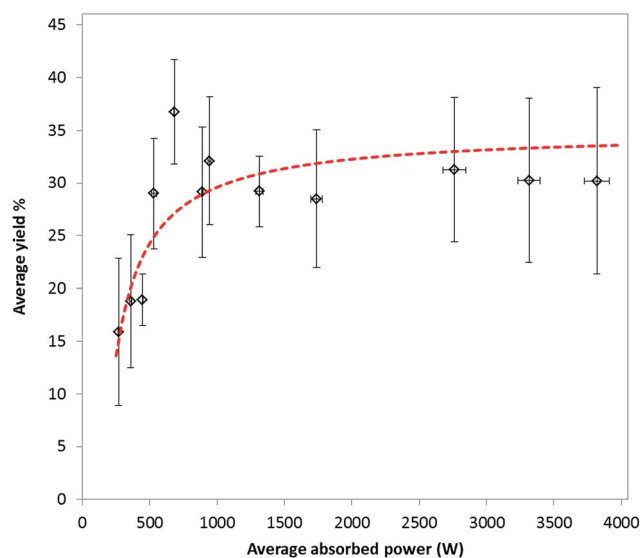


Fig. 2 Plot of average absorbed power vs. average yield of MIL-53(Al)*ta* (black diamonds) at an energy of 51  $\text{kJ mol}^{-1}$ , based on water in the reaction mixture. Predicted yield based on multiple linear regression (red dotted line, see Experimental section for further details). A microwave frequency of 2.45 GHz was used. Error bars are plotted  $\pm$  one standard deviation.

the average absorbed power (average of the forward minus the reflected power) and total absorbed energy were calculated. A microwave frequency of 2.45 GHz was used, consistent with penetration depth measurements. After microwave irradiation, the reaction mixture was allowed to cool and the resulting white powder recovered by filtration, washed with deionised water (*ca.* 10 mL  $\times$  3) and dried in air. A minimum of three separate reactions were carried out at each power and energy. The yields of MIL-53(Al)*ta* were determined in triplicate using thermogravimetric analysis. Data are given in Table S3† and Fig. 2.

Regression analysis was used to develop a predictive model for the yield of MIL-53(Al). Analysis of variance (ANOVA) showed that the model is statistically significant, with  $p < 0.00001$ . Multiple linear regression (MLR) was used to determine the coefficients and significance of absorbed energy and treatment time for all experiments using 41 variables (degrees of freedom) in the final calculation. Absorbed energy was shown to be statistically significant with  $p < 0.05$ , as was time with  $p < 0.00001$ . The obtained MLR coefficients were used to model the yield at 18.7 kJ (the average energy input across all regressed experiments, *i.e.* 50.2  $\text{kJ mol}^{-1}$  based on water), at treatment times between 75 and 4.5 s, equivalent to average absorbed powers between 250 W and 4.0 kW, respectively. Results of the modelled yield are plotted as a function of average absorbed power in Fig. 2.

## Results and discussion

Previous studies on the effect of microwave heating on the synthesis of MOFs have involved measurement of the average temperature of the reaction mixture using ruby thermometers, infra-red or fibre optic sensors.<sup>14,16</sup> These approaches do not



take into account the effect of localised microwave heating and simply measure average bulk temperature resulting from the differential heating of individual phases coupled with subsequent heat transfer. In this work we investigate the mechanism of MOF formation by studying the effect of delivering 56 kJ mol<sup>-1</sup> (based on water solvent) to an appropriate reaction mixture to make MIL-53(Al). The microwave power was varied between 250 and 4000 W, and time was varied appropriately to keep the total energy delivered constant.

### Effect of average absorbed power on yield of MIL-53(Al)*ta*

At all powers, reaction of [Al<sub>2</sub>(SO<sub>4</sub>)<sub>3</sub>] · 18H<sub>2</sub>O with H<sub>2</sub>BDC in water in a ratio of 1 : 1 at 0.17 mol dm<sup>-3</sup> concentration in our microwave system gave the as-synthesised phase containing both MIL-53(Al)*ta* and MIL-53(Al)*op*. MIL-53(Al)*ta* phase is common and arises from trapping of uncoordinated H<sub>2</sub>BDC within the pores of the MOF. Removal of H<sub>2</sub>BDC leads to a phase change to a more open structure, MIL-53(Al)*op* which is the more porous phase. We did not see a difference in the amount of occluded H<sub>2</sub>BDC with varying microwave power (Table S3†). MIL-53(Al)*op* converts to the hydrated form, MIL-53(Al)*hy*, upon adsorption of water. Powder X-ray diffraction (PXRD) analyses of products obtained from reactions at each power exhibit no peaks corresponding to impurities γ-AlO(OH) or other MOF phases beyond MIL-53(Al) (Fig. S2 and S3†).

Fig. 2 shows the effect of the average absorbed power upon the average yield of MIL-53(Al)*ta* at a total absorbed energy of 51 kJ mol<sup>-1</sup>. It should be noted that although the target energy was 56 kJ mol<sup>-1</sup>, owing to rapid changes in the dielectric properties of the reaction mixture during microwave irradiation, the match parameters varied significantly and so the average energy absorbed by the reaction mixture experimentally was approximately 51 kJ mol<sup>-1</sup> based on water. A rapid increase in yield of MIL-53(Al)*ta* from 15.9 ± 7.0 to 36.8 ± 4.9% between average absorbed powers of 269 ± 2 and 682 ± 4 W is observed. This trend of increasing yield with increasing power at constant energy shows that a selective heating mechanism of the aqueous metal ions in solution is taking place during the microwave treatment.<sup>20</sup> In particular, treatments involving higher powers and shorter reaction times result in highly localised heating whereby the rate of heating is greater than the loss of heat through dissipation,<sup>24</sup> thus increasing the overall rate of reaction. At powers above 682 ± 4 W the yield of MIL-53(Al)*ta* does not increase above ca. 30%. We ascribe the levelling off in yield at 30% to the stoichiometry of the reagents and hence diminishing availability of Al(III) during the reaction. Recently Taddei *et al.* reported no conversion of reactants using the same ratio as that used in our study, *i.e.* 1 : 1 of Al<sub>2</sub>(SO<sub>4</sub>)<sub>3</sub> : H<sub>2</sub>BDC.<sup>25</sup>

### Effect of average absorbed power on MIL-53(Al)*ta* particle size and morphology

Generally, microwave heating gives rise to smaller, well-defined MOF crystals compared with conventional heating.<sup>12</sup> The formation of many small crystals (<5 μm) throughout the bulk of the solution has previously been ascribed to local superheating of the solvent giving hotspots from which the crystals nucleate.<sup>13</sup>

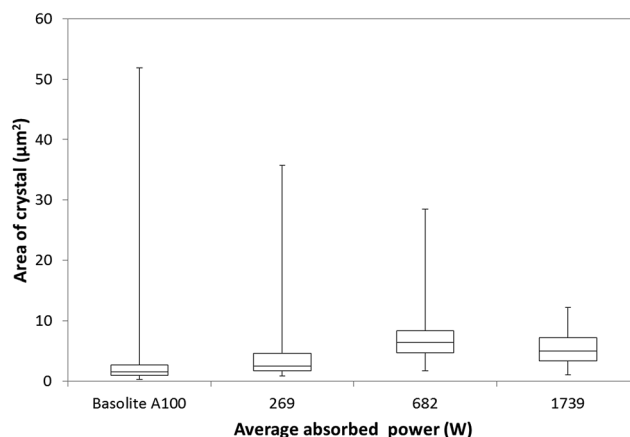


Fig. 3 Box and whisker plot of average absorbed power vs. particle size of MIL-53(Al)*ta* and commercial material Basolite A100 from SEM analyses. Error bars represent the largest and smallest particle sizes. Boxes represent the interquartile range (outer line) and median (central line) particle sizes.

Using the particle size distribution analysis method of Tsai and Langner,<sup>26</sup> our present work shows that both particle size range and morphology of MIL-53(Al)*ta* can be controlled by altering the microwave power (Fig. 3). As the average absorbed power increases the range of particle sizes observed by scanning electron microscopy (SEM) analysis becomes much narrower. For example, a median particle size of 2 μm<sup>2</sup> with a range between 0.9 and 36 μm<sup>2</sup> is exhibited by MIL-53(Al)*ta* particles synthesised at 269 ± 2 W. However, particle sizes recovered from reaction at a power of 1739 ± 44 W have a median size of 5 μm<sup>2</sup> with a range between 1 and 12 μm<sup>2</sup>, as identified by SEM analysis. Interestingly, a change in morphology of particles with power is also observed in the SEM images. At an average absorbed power of 269 ± 2 W the recovered MIL-53(Al)*ta* is composed of a 50 : 50 mixture of irregular-shapes and well-defined cubes (Fig. S8 and S9†). As the microwave power increases the ratio of morphologies shifts in favour of formation of well-defined cubes. For example, at an average absorbed power of 1739 ± 44 W the ratio of irregular-shapes to well-defined cubes is 10 : 90 (Fig. S8–S11†). Particle formation may be a consequence of two different growth mechanisms which are affected by several factors including, but not limited to, reaction kinetics, dissolution of H<sub>2</sub>BDC and temperature.<sup>27</sup>

One of the future goals of this work is to develop a procedure for producing industrially meaningful quantities of MOF, and therefore we have compared materials produced using our current method with the current industrial standard for MIL-53(Al) (Basolite A100). SEM image analysis of commercially available MIL-53(Al) material (Basolite A100) shows that it is most similar to MIL-53(Al)*ta* prepared in water at 269 ± 2 W (Fig. 3, S8 and S12†), and is composed of large aggregates of irregular shaped particles with a median particle size of 1.5 μm<sup>2</sup>. The range of particle sizes is very broad, between 0.3 and 52 μm<sup>2</sup>. The irregular shape and lower median particle size exhibited by Basolite A100 leads to broadening of the peaks in the PXRD pattern (Fig. S3 and S4†). Using the method of Vivani



**Table 1** Summary of relative crystallinity of MIL-53(Al). The more crystalline the material, the higher the value of 1/full width half maximum

Average absorbed power (W)	Relative crystallinity (1/FWHM)
Basolite A100	1.79
269 ± 2	5.20
682 ± 4	4.31
945 ± 11	4.76
1739 ± 44	5.17
3819 ± 92	4.46

*et al.* the reciprocals of the full width half maximum (1/FWHM) for a selected peak in the PXRD pattern were compared<sup>15</sup> (Table 1). FWHM were determined using a split pseudo-Voigt peak fitting function (Fig. S4†). The relative crystallinity 1/FWHM remained consistently between 4 and 6 for materials synthesised using microwave heating, whereas Basolite A100 exhibited low crystallinity (1/FWHM = 2). These data show that microwave heating offers a clear advantage over conventional heating processes for preparation of materials.

#### Effect of average absorbed power on MIL-53(Al)*op*

In order to study the porosity of materials produced using microwave heating, H<sub>2</sub>BDC was removed from the as-synthesised MIL-53(Al)*ta* by sublimation, giving the open structure, MIL-53(Al)*op*. A summary of data from N<sub>2</sub> gas sorption in MIL-53(Al)*op* is provided in Table 2. Samples of MIL-53(Al)*op* prepared by microwave heating in this study exhibit type I isotherms for N<sub>2</sub> uptake with very little hysteresis. Basolite A100 displays a type I/IV isotherm with greater hysteresis than the microwave-synthesised materials, indicative of interparticulate mesoporosity. Comparison of the relative microporosity of MIL-53(Al)*op* materials prepared by microwave heating with the commercial material was achieved using the ratio of the pore volume at low pressure to the pore volume at high relative pressure ( $V_{0.1}/V_{Tot}$ ).<sup>28</sup> Values of  $V_{0.1}/V_{Tot}$  that tend towards one are indicative of highly microporous materials, and the results summarised in Table 2 confirm that all microwave-synthesised materials have consistently high  $V_{0.1}/V_{Tot}$  ratios

equal to or above 0.8. Basolite A100, however, exhibits lower microporosity with a ratio of  $V_{0.1}/V_{Tot}$  at 0.4. These data are consistent with both SEM image analyses and a report in which nanoscale crystals of MIL-53 with large aggregation exhibit high total pore volumes ( $V_{Tot}$ ) arising from intergranular pores,<sup>29</sup> with aggregation reported to be highly dependent on the solvent used during synthesis.

Data in Table 2 show no obvious functional form to the correlation between microwave power and surface area. Materials prepared at powers of 269, 682 and 1739 W all exhibit Brunauer–Emmett–Teller surface areas ( $SA_{BET}$ ) within the range of MIL-53(Al)*op* materials prepared *via* conventional heating in continuous flow (459–919 m<sup>2</sup> g<sup>−1</sup>).<sup>22</sup> The highest  $SA_{BET}$  of 970 m<sup>2</sup> g<sup>−1</sup> was exhibited by MIL-53(Al)*op* synthesised at 682 ± 4 W. This  $SA_{BET}$  is higher than both the commercial Basolite A100 material (834 m<sup>2</sup> g<sup>−1</sup>) and MIL-53(Al)*op* synthesised by continuous flow (919 m<sup>2</sup> g<sup>−1</sup>).<sup>22</sup> MIL-53(Al)*op* produced at 3819 ± 92 W gave the lowest  $SA_{BET}$  for our materials at 280 m<sup>2</sup> g<sup>−1</sup>. We ascribe this reduction in  $SA_{BET}$  at high power to material degradation as a result of elevated bulk reaction temperatures as the amount of Al was higher than expected in the thermogravimetric data (Table S3†) and no metal oxide was observed in the PXRD patterns. In addition, the reduction in  $SA_{BET}$  is consistent with a previous report in which microwave synthesis of MOF-5 at powers above 1000 W led to deterioration of crystal quality and reduction in porosity.<sup>16</sup>

#### Synthesis of MIL-53(Al)*ta* in 4.3 seconds

In addition to our study on the effect of energy delivery on the formation of MIL-53(Al), we have developed a procedure for the synthesis of MOFs in unprecedentedly short time-scales. Rapid synthesis of MOFs is often limited to coordination complexes that are easily accomplished,<sup>13,29</sup> or demonstrated at room temperature.<sup>30,31</sup> Using our approach the synthesis of *ca.* 62 mg of MIL-53(Al)*ta* in 4.3 seconds was achieved by exposing the reaction mixture in a solvothermal vessel to an average absorbed power of 3819 ± 92 W. A yield of *ca.* 30 ± 8% comparable with literature reports using the same ratio of metal : ligand and water as the solvent was obtained,<sup>22,25</sup> but the reaction time is much reduced (normally 3 days *via* solvothermal routes<sup>17</sup> or 6 minutes in continuous flow<sup>22</sup>). As described above it is possible

**Table 2** Summary of gas sorption data collected at 77 K using N<sub>2</sub> as the sorbate

Average absorbed power (W)	Langmuir surface area <sup>a,b</sup> (m <sup>2</sup> g <sup>−1</sup> )	BET surface area <sup>a,c</sup> (m <sup>2</sup> g <sup>−1</sup> )	Micropore volume <sup>d</sup> ( $V_{0.1}$ )	Total pore volume <sup>e</sup> ( $V_{Tot}$ )	$V_{0.1}/V_{Tot}$
<b>Commercial material<sup>f</sup></b>	<b>864</b>	<b>834</b>	<b>0.35</b>	<b>0.88</b>	<b>0.40</b>
269 ± 2	685	658	0.24	0.27	0.89
682 ± 4	1020	970	0.35	0.44	0.79
945 ± 11	458	436	0.16	0.19	0.84
1739 ± 44	513	504	0.18	0.22	0.81
3819 ± 92	285	280	0.10	0.12	0.83

<sup>a</sup> Values given to zero decimal places. <sup>b</sup>  $P/P_0$  range 0.001 to 0.01. <sup>c</sup> In order to achieve positive values for  $C$  for the BET surface area, the Rouquerol plot was used in the  $P/P_0$  range 0.001 to 0.01. <sup>d</sup> Pore volume at  $P/P_0 = 0.1$  derived from the Dubinin–Astakhov equation. <sup>e</sup> Total pore volume at  $P/P_0 = 0.99$ . <sup>f</sup> Values are given to two decimal places. <sup>g</sup> Basolite A100 obtained from Sigma Aldrich. Values in italics and bold are within the reported range of MIL-53(Al)*op* materials prepared *via* conventional heating in continuous flow.<sup>22</sup>





to improve the yield of MIL-53(Al)*ta* by altering the ratio of metal salts and carboxylic ligand, but our current experimental set-up is limited by the reduced penetration depths observed for more concentrated metal salt solutions. We are currently working towards modifying our experimental set-up to overcome these limitations thus enabling use of various solvents and the possibility of even faster MOF syntheses. In this paper we have significantly reduced the synthesis time of MIL-53(Al) using microwave heating. However, it is still necessary to remove occluded H<sub>2</sub>BDC from the pores of MIL-53(Al)*ta* in order to give the open framework. Future work includes investigating methods of efficient H<sub>2</sub>BDC removal.

## Conclusions

In this work the amount of energy absorbed by a MOF reaction mixture during microwave irradiation has, for the first time, been experimentally quantified and used to examine the effect of average absorbed power at constant total absorbed energy on the yield and properties of MIL-53(Al). We have identified a selective heating mechanism in MOF syntheses by increasing microwave power with fixed total absorbed energy that leads to rapid synthesis and higher yields (30% at 3819 W *cf.* 16% at 269 W) of MIL-53(Al). Furthermore, we have confirmed that both the MIL-53(Al) particle size range and morphology can be controlled by altering microwave power. Microwave-synthesised materials are microporous, exhibiting type I nitrogen gas sorption isotherms. MIL-53(Al) produced at  $682 \pm 4$  W displays a  $S_{\text{ABET}}$  of  $970 \text{ m}^2 \text{ g}^{-1}$  which is higher than the commercial Basolite A100 material and MIL-53(Al) synthesised by continuous flow (both prepared *via* conventional heating processes).<sup>13,22</sup> A procedure for the microwave synthesis of MOFs in unprecedented time-scales has also been developed and is demonstrated by synthesis of *ca.* 62 mg of MIL-53(Al) in 4.3 seconds and is the fastest reported synthesis of a MOF in bulk on this scale to date. This procedure further demonstrates the ability of microwave technology to prepare MOFs in bulk at times significantly faster than by conventional heating methods.

## Statement of contribution

AL, JK, RSFJ: designed and built microwave equipment and carried out synthesis, CGM, SY: PXRD and relative crystallinity characterisation, AL: TGA and gas sorption analyses, OU: imaging of MOF materials, TLE: spectroscopic analysis, AL, CD, SWK, NRC, MS: designed and supervised project and developed protocols, all authors: contributed to writing of manuscript.

## Acknowledgements

We thank the EPSRC (EP/I011870, EP/I020942) for support. MS acknowledges support from the ERC for an Advanced Grant (AdG 226593). AL acknowledges the University of Nottingham for the award of Nottingham Research Fellowship. NRC acknowledges the receipt of a Royal Society Wolfson Merit

Award. TLE acknowledges the Royal Society for the award of a University Research Fellowship.

## Notes and references

- 1 G. Férey, *Chem. Soc. Rev.*, 2008, **37**, 191.
- 2 H. Furukawa, K. E. Cordova, M. O'Keeffe and O. M. Yaghi, *Science*, 2013, **341**, 974; S. Yang, A. J. Ramirez-Cuesta, R. Newby, V. Garcia-Sakai, P. Manuel, S. K. Callear, S. I. Campbell, C. C. Tang and M. Schröder, *Nat. Chem.*, 2015, **7**, 121.
- 3 J.-R. Li, R. J. Kuppler and H.-C. Zhou, *Chem. Soc. Rev.*, 2009, **38**, 1477; T. L. Easun, F. Moreau, Y. Yan, S. Yang and M. Schröder, *Chem. Soc. Rev.*, 2017, **46**, 239.
- 4 D. Farrusseng, S. Aguado and C. Pinel, *Angew. Chem., Int. Ed.*, 2009, **48**, 7502.
- 5 M. Dan-Hardi, C. Serre, T. Frot, L. Rozes, G. Maurin, C. Sanchez and G. Férey, *J. Am. Chem. Soc.*, 2009, **131**, 10857.
- 6 A. Morozan and F. Jaouen, *Energy Environ. Sci.*, 2012, **5**, 9269.
- 7 N. Stock and S. Biswas, *Chem. Rev.*, 2012, **112**, 933.
- 8 M. Gaab, N. Trukhan, S. Maurer, R. Gummaraju and U. Müller, *Microporous Mesoporous Mater.*, 2012, **157**, 131.
- 9 M. Klimakow, P. Klobes, A. F. Thuenemann, K. Rademann and F. Emmerling, *Chem. Mater.*, 2010, **22**, 5216.
- 10 A. M. Joaristi, J. Juan-Alcaniz, P. Serra-Crespo, F. Kapteijn and J. Gascon, *Cryst. Growth Des.*, 2012, **12**, 3489.
- 11 N. A. Khan and S. H. Jhung, *Coord. Chem. Rev.*, 2015, **285**, 11.
- 12 J. Klinowski, F. A. Almeida Paz, P. Silva and J. Rocha, *Dalton Trans.*, 2011, **40**, 321.
- 13 Z. Ni and R. I. Masel, *J. Am. Chem. Soc.*, 2006, **128**, 12394.
- 14 S. H. Jhung, J.-H. Lee, P. M. Forster, G. Férey, A. K. Cheetham and J.-S. Chang, *Chem.-Eur. J.*, 2006, **12**, 7899; Y. K. Hwang, J.-S. Chang, S.-E. Park, D. S. Kim, Y.-U. Kwon, S. H. Jhung, J.-S. Hwang and M. S. Park, *Angew. Chem., Int. Ed.*, 2005, **44**, 556.
- 15 M. Taddei, P. V. Dau, S. M. Cohen, M. Ranocchiari, J. A. van Bokhoven, F. Costantino, S. Sabatini and R. Vivani, *Dalton Trans.*, 2015, **44**, 14019.
- 16 N. A. Khan, E. Haque and S. H. Jhung, *Phys. Chem. Chem. Phys.*, 2010, **12**, 2625; J.-S. Choi, W.-J. Son, J. Kim and W.-S. Ahn, *Microporous Mesoporous Mater.*, 2008, **116**, 727.
- 17 C. Serre, F. Millange, C. Thouvenot, M. Noguès, G. Marsolier, D. Louër and G. Férey, *J. Am. Chem. Soc.*, 2002, **124**, 13519.
- 18 E. Haque, J. H. Jeong and S. H. Jhung, *CrystEngComm*, 2010, **12**, 2749–2754; E. Haque, N. A. Khan, J. H. Park and S. H. Jhung, *Chem.-Eur. J.*, 2010, **16**, 1046.
- 19 S. Bourrelly, P. L. Llewellyn, C. Serre, F. Millange, T. Loiseau and G. Férey, *J. Am. Chem. Soc.*, 2005, **127**, 13519.
- 20 A. Laybourn, J. Katrib, P. A. Palade, T. L. Easun, N. R. Champness, M. Schröder and S. W. Kingman, *Phys. Chem. Chem. Phys.*, 2016, **18**, 5419.
- 21 A. C. Metaxas and R. J. Meredith, *Industrial Microwave Heating*, Peter Peregrinus Ltd., London, UK, 1983.
- 22 P. A. Bayliss, I. A. Ibarra, E. Perez, S. Yang, C. C. Tang, M. Poliakoff and M. Schroder, *Green Chem.*, 2014, **16**, 3796; I. A. Ibarra, P. Bayliss, E. Pérez, S. Yang, A. J. Blake, H. Nowell, D. R. Allan, M. Poliakoff and M. Schröder, *Green Chem.*, 2012, **14**, 117.



- 23 G. F. Engen, *IEEE Trans. Microwave Theory Tech.*, 1997, **45**, 2414.
- 24 D. N. Whittles, S. W. Kingman and D. J. Reddish, *Int. J. Miner. Process.*, 2003, **68**, 71; S. R. Vallance, S. Kingman and D. H. Gregory, *Adv. Mater.*, 2007, **19**, 138.
- 25 M. Taddei, D. A. Steitz, J. A. Van Bokhoven and M. Ranocchiari, *Chem.-Eur. J.*, 2016, **22**, 3245.
- 26 C.-W. Tsai and E. H. G. Langner, *Microporous Mesoporous Mater.*, 2016, **221**, 8.
- 27 C. Carlucci, H. Xu, B. F. Scremin, C. Giannini, D. Altamura, E. Carlino, V. Videtta, F. Conciauro, G. Gigli and G. Ciccarella, *CrystEngComm*, 2014, **16**, 1817.
- 28 X. Cheng, A. Zhang, K. Hou, M. Liu, Y. Wang, C. Song, G. Zhang and X. Guo, *Dalton Trans.*, 2013, **42**, 13698.
- 29 R. Dawson, A. Laybourn, R. Clowes, Y. Z. Khimyak, D. J. Adams and A. I. Cooper, *Macromolecules*, 2009, **42**, 8809.
- 30 D. Tanaka, A. Henke, K. Albrecht, M. Moeller, K. Nakagawa, S. Kitagawa and J. Groll, *Nat. Chem.*, 2010, **2**, 410; Y. Yoo and H.-K. Jeong, *Chem. Commun.*, 2008, 2441.
- 31 D. J. Tranchemontagne, J. R. Hunt and O. M. Yaghi, *Tetrahedron*, 2008, **64**, 8553.

